



# Émission d'ondes internes par une sphère oscillant horizontalement en fluide uniformément stratifié

Evgueni Ermanyuk, Jan-Bert Flor, Bruno Voisin

## ► To cite this version:

Evgueni Ermanyuk, Jan-Bert Flor, Bruno Voisin. Émission d'ondes internes par une sphère oscillant horizontalement en fluide uniformément stratifié. CFM 2009 - 19ème Congrès Français de Mécanique, Aug 2009, Marseille, France. <hal-03391271>

**HAL Id: hal-03391271**

**<https://hal.science/hal-03391271v1>**

Submitted on 21 Oct 2021

**HAL** is a multi-disciplinary open access archive for the deposit and dissemination of scientific research documents, whether they are published or not. The documents may come from teaching and research institutions in France or abroad, or from public or private research centers.

L'archive ouverte pluridisciplinaire **HAL**, est destinée au dépôt et à la diffusion de documents scientifiques de niveau recherche, publiés ou non, émanant des établissements d'enseignement et de recherche français ou étrangers, des laboratoires publics ou privés.



HAL Authorization

# Internal wave radiation by a horizontally oscillating sphere in a uniformly stratified fluid

E. V. ERMANYUK<sup>1</sup>, J.-B. FLÓR, B. VOISIN

Laboratoire des Écoulements Géophysiques et Industriels (LEGI), CNRS–UJF–GINP,  
BP 53, 38041 GRENOBLE

## Résumé :

*On présente une méthode expérimentale et une théorie inédites pour l'émission des ondes internes de gravité par une sphère oscillant horizontalement dans un fluide linéairement stratifié. La théorie, linéaire, considère des petites perturbations tridimensionnelles et incorpore les effets visqueux et transitoires ainsi que les effets de masse ajoutée et de champ proche. La méthode expérimentale mesure l'amplitude et la structure des ondes par visualisation d'encre fluorescente dans un plan vertical. Elle permet à la fois des visualisations attrayantes et des mesures précises, et contrairement aux méthodes existantes elle donne accès à chaque section verticale du champ d'onde. La théorie champ proche est en excellent accord avec les résultats expérimentaux, les résultats expérimentaux antérieurs s'étant avérés brouillés par les réflexions d'ondes et les régimes transitoires. Un accroissement de l'amplitude d'oscillation montre que la théorie demeure précise à plus de 5% tant que l'amplitude relative d'oscillation vérifie  $A/D < 0.1$  avec  $D$  le diamètre de la sphère.*

## Abstract :

*We present a new experimental method and theory for the internal wave field emitted by a horizontally oscillating sphere in a linearly stratified fluid. The linear theory is for small-amplitude three-dimensional perturbations and incorporates viscous effects, transient effects, added-mass effects and near-field effects. For the measurements of the wave amplitude and structure, we employ a dye visualization technique in a single vertical plane. This technique allows simultaneously for appealing flow visualizations and accurate wave measurements, and in contrast to other methods allows for the measurement across a single vertical section. The near-field approximation of the theory is found to be in excellent agreement with the experimental results, in contrast to former experimental results in which wave reflection and transient effects obscured the comparison. Increasing the oscillation amplitude shows that linear theory is accurate up to 5% when the non-dimensional oscillation amplitude is  $A/D < 0.1$  where  $D$  is the sphere diameter.*

**Mots clefs :** internal waves, oscillating sphere, stratified fluids, tidal waves

## 1 Introduction

Internal waves are generated in the ocean due to tidal motion over topography, and dissipate up to 25% of the total tidal energy [1, 2]. This internal wave energy is either absorbed into the mean flow by wave–mean–flow interactions, or dissipated by mixing and small-scale viscous effects. Therefore, it plays an important role in climate models. In this paper we consider the idealized case of a horizontally oscillating object, and the structure and amplitude of the wave field emitted. For the object we take a sphere for which the wave pattern is three-dimensional. The stratification is taken linear. Details on the experiments and theory are given in [3].

The radiation of internal waves by an oscillating object is a classical problem of fluid mechanics, discussed e.g. in Lighthill's book on waves [4]. Experimental observations of wave rays emitted by an oscillating circular horizontal cylinder [5, 6] have revealed the now well-known St Andrew's Cross pattern of rays. The dispersion relation of the waves predicts the angle of the rays with the horizontal as a function of the buoyancy frequency,  $N$ , and the frequency of oscillation,  $\omega$ . But the wave structure and amplitude in space and time are to be further investigated. Also the three-dimensional wave structure, as emitted by more complex oscillating objects, requires further study.

<sup>1</sup>Permanent affiliation: Lavrentyev Institute of Hydrodynamics, Siberian Division of the Russian Academy of Science, Prospekt Lavrentyev 15, NOVOSIBIRSK 630090 (RUSSIA)

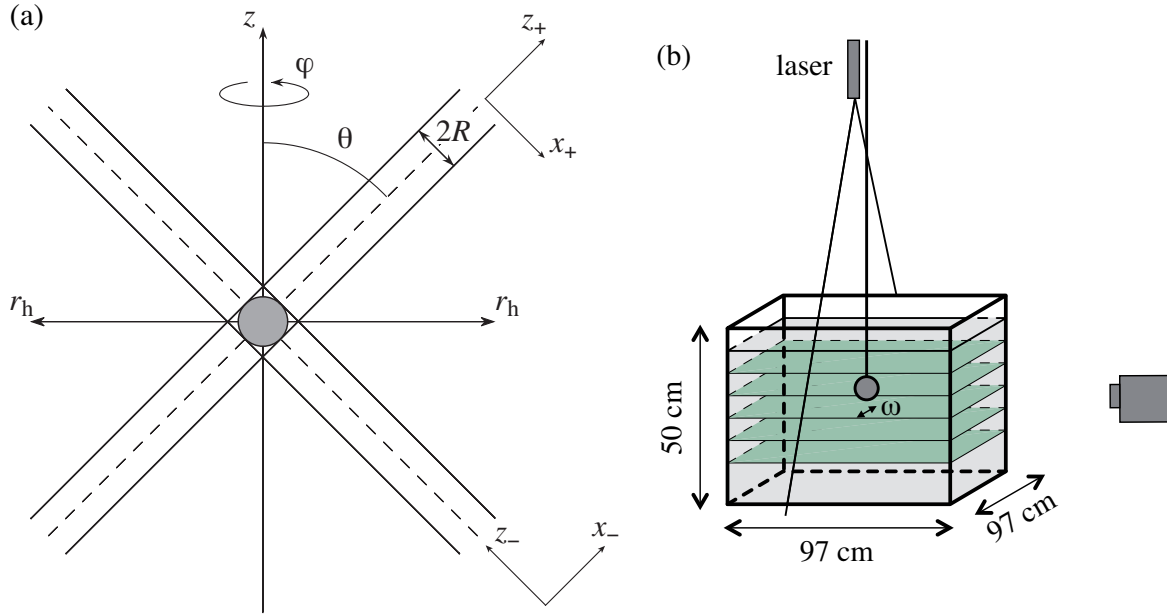


FIG. 1 – (a) Wave field geometry and (b) experimental set-up.

Hurley [7] considered inviscid internal wave radiation by an oscillating elliptical horizontal cylinder (with its major axis inclined to the horizontal) and the cross-beam particle displacements in the wave rays, and Hurley and Keady [8] included viscous effects. They have shown that the cross-beam profile is the same for all ellipse shapes and that, depending on distance from the cylinder and Reynolds–Stokes number, it exhibits a bimodal or unimodal form, characterized by an envelope with twin or single maximum, respectively, as first recognized by Makarov et al. [9]. This theory was successfully compared to experiments by Sutherland and collaborators [10, 11, 12] and Zhang et al. [13]. In addition it was extended to the axisymmetric case of a vertically oscillating sphere by Flynn et al. [14]. In contrast to the excellent agreement between theory and experiment found for the oscillating cylinder, the comparison of theory and experiment for the oscillating sphere showed significant scatter in the wave profiles. It was this discrepancy which led to the present study, consisting in development of a new theory and realization of new experiments that are described in more detail in [3].

The theory builds further on Hurley [7] and Hurley and Keady [8] and is an extension of earlier work by Voisin [15]. In particular the included added mass effect has an important influence on the radiated wave power [16, 17, 18] which is of interest to oceanographic applications [2]. In this paper we will only give the main lines of the theory for the near and far wave field of a horizontally oscillating sphere.

## 2 Theory

In an unbounded Boussinesq fluid of kinematic viscosity  $\nu$ , uniformly stratified with buoyancy frequency  $N$ , a rigid sphere of radius  $R$  starts at time  $t = 0$  to oscillate horizontally at the frequency  $\omega < N$  with amplitude  $A \ll R$ . In Cartesian coordinates  $(x, y, z)$  with the  $z$ -axis vertical and the  $x$ -axis directed along the oscillations, the position of the centre of the sphere is written as  $(A, 0, 0) \sin(\omega t + \Theta)$ . Internal waves are generated which propagate at the angle  $\theta = \arccos(\omega/N)$  to the vertical, on a double cone with apex at the sphere. This cone is the three-dimensional analogue of the two-dimensional St Andrew’s Cross. Wave beams are formed inside the conical shell delimited by the double cones tangent to the sphere above and below, as illustrated in figure 1a. Their structure is governed by two dimensionless parameters: the product  $\omega t$  characterizing the number of periods elapsed since the start-up, and the Reynolds–Stokes number

$$Re = \frac{2\omega R^2}{\nu}, \quad (1)$$

characterizing the ratio of the radius  $R$  of the sphere to the thickness  $(2\nu/\omega)^{1/2}$  of the viscous boundary layer at its surface. In the following both are assumed large, such that  $\omega t \gg 1$  and  $Re \gg 1$ , allowing the steady inviscid wave beams to form before being affected by unsteadiness and viscosity as the waves propagate away.

The near field is the region  $r/R = O(1)$  close to the sphere where the wave beams intersect and merge, with

$r = |\mathbf{x}|$ . It is more appropriately described in cylindrical coordinates  $(r_h, \varphi, z)$ . In complex notation the vertical displacement  $\zeta$  of fluid particles may be expressed for any  $r/R$  as

$$\frac{\zeta}{A} = \pm 2i \cos^3 \theta \frac{\cos \varphi}{1 + B(\cos \theta)} e^{-i(\omega t + \Theta)} \times \int_0^{\cos \theta / (\alpha |Z|)} \exp\left(-\frac{\beta K^3 |Z|}{\cos \theta}\right) j_1(K) J_1(K R_h \cos \theta) \exp(-iK|Z| \sin \theta) K dK, \quad (2)$$

where  $j_1(x) = [\pi/(2x)]^{1/2} J_{3/2}(x) = (\sin x)/x^2 - (\cos x)/x$  is a spherical Bessel function. Position has been nondimensionalized as  $\mathbf{X} = \mathbf{x}/R$ , and the upper sign is used in the upper half-space and the lower sign in the lower half-space so that  $\pm = \text{sign } z$ . The term

$$B(\cos \theta) = \cos^2 \theta \left\{ 1 - \sin \theta \left[ \text{arctanh}(\sin \theta) + i \frac{1}{2} \pi \right] \right\}, \quad (3)$$

equal to  $1/3$  in a homogeneous fluid, represents the effect of the stratification on the added mass of the sphere, while the two parameters

$$\alpha = \frac{1}{\omega t \tan \theta}, \quad \beta = \frac{1}{R \tan \theta}, \quad (4)$$

both small, represent the effects of unsteadiness and viscosity on the waves, respectively.

Outside the near field, the wave beams separate and a description in conical polar coordinates  $(x_{\pm}, \varphi, z_{\pm})$  is more appropriate, illustrated in figure 1a and such that

$$x_{\pm} = r_h \cos \theta \mp z \sin \theta, \quad z_{\pm} = \pm r_h \sin \theta + z \cos \theta, \quad (5)$$

with  $|z_{\pm}|$  the along-beam coordinate and  $x_{\pm}$  the cross-beam coordinate. The far field is the region  $|z_{\pm}| \gg 1$  with  $|x_{\pm}| = O(1)$ . There, the vertical displacement simplifies to

$$\frac{\zeta}{A} \sim \pm \frac{\cos^{5/2} \theta}{\sin^{1/2} \theta} \frac{\cos \varphi}{1 + B(\cos \theta)} \frac{e^{-i(\omega t + \Theta + \pi/4)}}{|Z_{\pm}|^{1/2}} \int_0^{1/(\alpha |Z_{\pm}|)} \exp(-\beta K^3 |Z_{\pm}|) J_{3/2}(K) \exp(iK x_{\pm}) dK. \quad (6)$$

The stability variation  $\Delta N^2 = -N^2 \partial \zeta / \partial z$  which is the quantity measured by the popular synthetic Schlieren technique used by Sutherland and collaborators [10, 11, 12, 14] follows immediately from multiplying the integrands of both formulae by  $\pm i(N^2/R)K \sin \theta$ .

### 3 Experimental set-up and measurement method

Experiments were conducted in a plexiglas square tank of working depth 50 cm and horizontal dimensions  $97 \times 97 \text{ cm}^2$ , represented in figure 1b. The tank was filled to a depth of 47 cm with a linearly stratified fluid of kinematic viscosity  $\nu = 0.012 \text{ cm}^2/\text{s}$ . Salt was used as stratifying agent and tap water as working fluid. The stratification was measured by taking density samples at different heights in the fluid, and the buoyancy frequency was kept constant in all experiments at  $N = 1.22 \text{ rad/s}$ . The waves were generated by a horizontally oscillating plexiglass sphere of radius  $R = 3.125 \text{ cm}$  attached to a pendulum of length  $l = 1.3 \text{ m}$ . This pendulum oscillated by means of a wheel placed at mid-height, rotating around an eccentric axis. The pendulum was pushed against the wheel by means of a counterweight mounted near the pivot. The oscillation amplitude  $A$  of the sphere was kept small compared to the length of the pendulum ( $A/l < 0.016$ ), and the motion was in good approximation horizontal. After 10 oscillation periods the wave pattern was steady. Measurements were taken after 20 oscillations.

The waves were visualized using the same method employed in Hopfinger et al. [19] for the measurement of waves and Flór et al. [20, 21] for the measurement of isopycnal displacements. A set of equidistant dye planes was generated by carefully displacing a rake of horizontally spanned – and in fluorescein solution soaked – cotton wires through the fluid. These planes were then illuminated with a vertical laser sheet at the position of the oscillating sphere. Molecular diffusion causes a Gaussian distribution of dye across each plane and is high during the first two hours (because of high gradients) and small at later times. The distance between adjacent dye planes was about 2 cm. The Gaussian dye distribution allows for the accurate measurement of the position of the centre of each plane, with subpixel resolution.

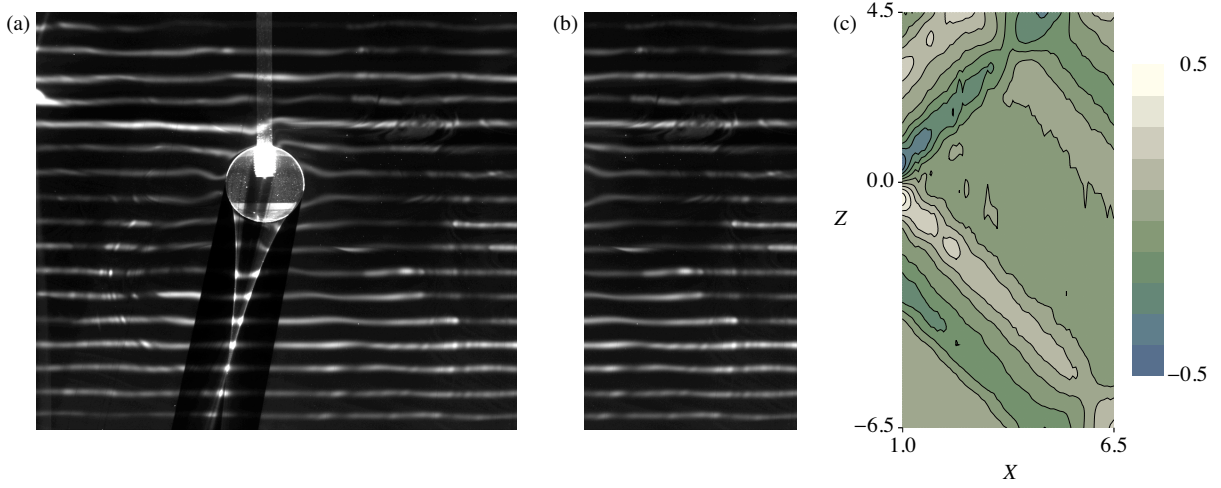


FIG. 2 – (a) Full image of the observed dye pattern and oscillating sphere, (b) processed portion of the image (to the right of the sphere) and (c) contour plot of normalized displacement differences  $\Delta\zeta/A$  obtained from two subsequent images. Distances are normalized with the sphere radius.

The light intensity  $I(z)$  across the dye planes along a vertical line thus varies as a sequence of Gaussian distributions. To determine the position of each maximum we suppose a standard Gaussian function, with its centre at  $z = z'$  and width  $2s$ ,

$$G(z, z', s) = \frac{1}{(2\pi)^{1/2}s} \exp \left[ -\frac{(z - z')^2}{2s^2} \right]. \quad (7)$$

The correlation of the experimental signal with a Gaussian peak of width  $2s_0$  is

$$C(z') = \int I(z) G(z, z', s_0) dz, \quad (8)$$

with the maximum of  $C(z')$  corresponding to the position of the Gaussian maximum in the signal. The correlation is calculated for discrete values with an increment of 1 pixel, i.e.  $C_k = \sum_{n=0}^{N-1} G_n I_{n+k}$ . To limit the calculation time the Gaussian function  $G(z, z', s)$  is calculated once for  $N$  points, with  $N = 4s_0$  to ensure that the tails of the function are sufficiently close to zero, and with centre  $z' = 2s_0$  i.e.  $G_n = G(n, 2s_0, s_0)$ . (A least-square approximation shows that the typical width of the Gaussians under experimental conditions is about 16 pixels so that  $s_0 = 8$ ). For the calculation of  $C(k)$  we thus displace the profile of  $I(z)$  with respect to the Gaussian function  $G_n$ . The values of  $C_k$  are used as the nodes for interpolation by cubic splines. Finally, the maxima of the interpolated curve are determined with an accuracy being set at 0.1 pixel. This accuracy corresponds to the estimated noise level in the experiments (based on dye plane thickness and picture quality), and can be as low as 0.03 pixel for thin dye planes. To reduce the noise and length of the calculations, for each line  $I(z)$  is taken an average over 6 vertical lines of pixels.

Figure 2 illustrates how this procedure has been applied to image pairs taken for a time increment  $\Delta t = 1$  s. For each pair the quantity  $\Delta\zeta(t) = \zeta(t + \Delta t) - \zeta(t)$  was obtained from the difference between the positions of the maxima of the correlation function. Considering the displacement difference instead of the instantaneous displacement filters out the noise which arises both from the drift in the electronic equipment and from the physical drift of the fluorescein lines. A similar filtering technique has been used by Sutherland and Linden [12] for a smaller time increment.

## 4 Experimental results and comparison with theory

Figure 3 shows the comparison between experiment and theory for oscillations of amplitude  $A/R = 0.109$  and frequency  $\omega = 0.905$  rad/s, yielding a Reynolds–Stokes number  $Re = 1470$ . The data, corresponding to figure 2, were measured in the analyzing window  $-5 < Z < 2.5$  and  $1 < X < 6$  in which the reflections of the wave beams are negligible. Each picture shows a series of four wave profiles, measured at intervals of 1 s starting 0.6 s after the pendulum has completed its twentieth oscillation, yielding on average  $\omega t = 130$ . Two vertical distances from the centre of the sphere are considered, one small  $Z = -1.44$  and the other larger  $Z = -4.08$ .

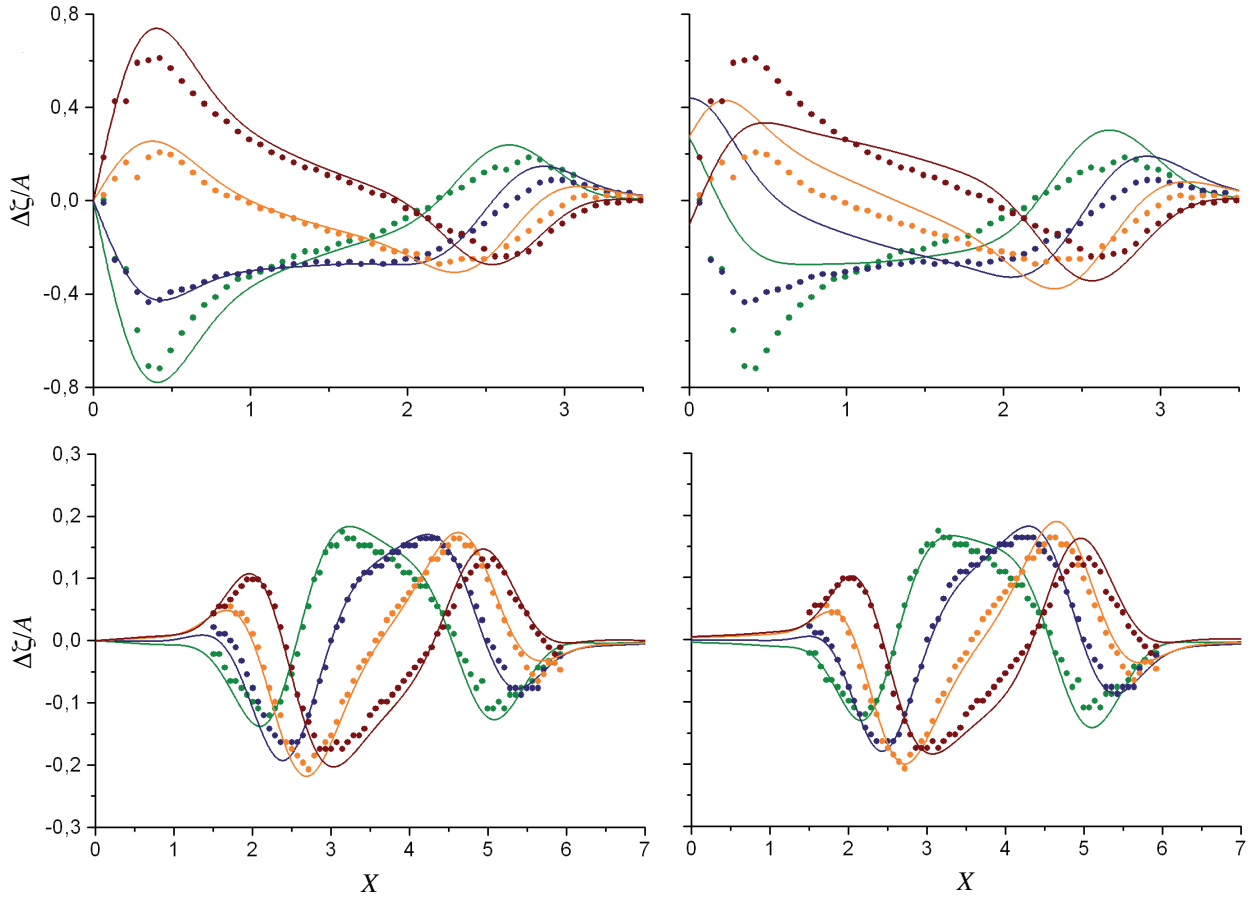


FIG. 3 – Comparison between theory and experiment, at  $Z = -1.44$  (top) and  $-4.08$  (bottom). The points and lines represent respectively the measurements and theory, with the near-field theory left and far-field theory right.

For the range of  $Z$ -values here considered, the near-field theory is in very good agreement with the experimental results. The far-field theory becomes valid only at sufficiently large  $|Z|$ . At the outer (inner) edge of the internal wave cone, the far-field theory slightly overestimates (underestimates) the wave motion. Only the near-field theory takes into account the increase of the ratio between the major-to-minor peaks of the wave envelope for decreasing values of  $|Z|$ . Accordingly, the near-field correction is particularly important near the sphere. For the top of an isolated topography in the ocean, this implies that the correct estimation of internal wave motion requires the use of the near-field theory.

## 5 Conclusions

The main conclusion is that there is a very good quantitative agreement between experimental results and the linear theory for the three-dimensional wave field generated by an oscillating sphere. Herewith we confirm that linear theory accurately predicts the wave radiation.

With the distance from the sphere, the influence of nearby generated waves decreases and the agreement of the far-field solution with the experimental results improves and is excellent beyond a distance of about three to four times the radius of the sphere. The inclusion of the effect of the stratification on the added mass of the sphere in the theory is found to improve the predicted wave amplitude by a non-negligible factor [3]. A thorough analysis of former experiments reported in the literature over the past decade (see [3]) suggests that the relevance of transient effects in the measurements has been ignored and can, in part, be considered responsible for biasing the agreement with the linear theory. Increasing the oscillation amplitude above  $A/R = 0.184$  reveals that for  $A/R \approx 0.5$  the amplitude exceeds the linear prediction by 20% whereas for larger oscillation amplitudes nonlinear wave radiation distorts the wave structure predicted according to linear theory [3].

In the Earth's oceans the principal region of internal wave generation is the continental slope. For typical tidal excursion 100 m and slope wider than 500 m linear theory applies. By contrast, typical slope heights from 1000 m to 2000 m and an ocean depth of 1000 m at the continental shelf (as reproduced in the laboratory by [22])

and [23]) imply that the far-field approach applies to a region that lays outside the domain of interest. Using the near-field theory would make a difference in wave amplitude of approximately 20 to 30% and is therefore much more accurate than the commonly used far-field approach.

Further, we have successfully exploited the dye-line technique of Hopfinger et al. [19] and Flór et al. [20, 21] for the quantitative and systematic measurement of internal wave fields. This technique provides high precision quantitative data that can compete with other methods, has the advantage to be accurate also in the very near field of the sphere, visualises nonlinear effects in the dye motion, and provides images that are readily interpretable. The details of this method are under investigation and will be presented elsewhere.

## References

- [1] Morozov E. G., Semidiurnal internal wave global field, *Deep-Sea Res. I*, 42, 135–148, 1995.
- [2] Garrett C. and Kunze E., Internal tide generation in the deep ocean, *Annu. Rev. Fluid Mech.*, 39, 57–87, 2007.
- [3] Voisin B., Ermanyuk E. V. and Flór J.-B., Internal wave generation by horizontal oscillation of a sphere, *J. Fluid Mech.*, submitted, 2009.
- [4] Lighthill J., *Waves in Fluids*, Cambridge University Press, 1978.
- [5] Mowbray D. E. and Rarity B. S. H., A theoretical and experimental investigation of the phase configuration of internal waves of small amplitude in a density stratified liquid, *J. Fluid Mech.*, 28, 1–16, 1967.
- [6] Thomas N. H. and Stevenson T. N., A similarity solution for viscous internal waves, *J. Fluid Mech.*, 54, 495–506, 1972.
- [7] Hurley D. G., The generation of internal waves by vibrating elliptic cylinders. Part 1. Inviscid solution, *J. Fluid Mech.*, 351, 105–118, 1997.
- [8] Hurley D. G. and Keady G., The generation of internal waves by vibrating elliptic cylinders. Part 2. Approximate viscous solution, *J. Fluid Mech.*, 351, 119–138, 1997.
- [9] Makarov S. A., Neklyudov V. I. and Chashechkin Yu. D., Spatial structure of two-dimensional monochromatic internal-wave beams in an exponentially stratified liquid, *Izv. Atmos. Ocean. Phys.*, 26, 548–554, 1990.
- [10] Sutherland B. R., Dalziel S. B., Hughes G. O. and Linden P. F., Visualization and measurement of internal waves by ‘synthetic schlieren’. Part 1. Vertically oscillating cylinder, *J. Fluid Mech.*, 390, 93–126, 1999.
- [11] Sutherland B. R., Hughes G. O., Dalziel S. B. and Linden P. F., Internal waves revisited, *Dyn. Atmos. Oceans*, 31, 209–232, 2000.
- [12] Sutherland B. R. and Linden P. F., Internal wave excitation by a vertically oscillating elliptical cylinder, *Phys. Fluids*, 14, 721–731, 2002.
- [13] Zhang H. P., King B. and Swinney H. L., Experimental study of internal gravity waves generated by supercritical topography, *Phys. Fluids*, 19, 096602, 2007.
- [14] Flynn M. R., Onu K. and Sutherland B. R., Internal wave excitation by a vertically oscillating sphere, *J. Fluid Mech.*, 494, 65–93, 2003.
- [15] Voisin B., Limit states of internal wave beams, *J. Fluid Mech.*, 496, 243–293, 2003.
- [16] Ermanyuk E. V., The rule of affine similitude for the force coefficients of a body oscillating in a uniformly stratified fluid, *Exps. Fluids*, 32, 242–251, 2002.
- [17] Ermanyuk E. V. and Gavrilov N. V., Force on a body in a continuously stratified fluid. Part 1. Circular cylinder, *J. Fluid Mech.*, 451, 421–443, 2002.
- [18] Ermanyuk E. V. and Gavrilov N. V., Force on a body in a continuously stratified fluid. Part 2. Sphere, *J. Fluid Mech.*, 494, 33–50, 2003.
- [19] Hopfinger E. J., Flór J.-B., Chomaz J.-M. and Bonneton P., Internal waves generated by a moving sphere and its wake in a stratified fluid, *Exps. Fluids*, 11, 255–261, 1991.
- [20] Flór J.-B., Ungarish M. and Bush J. W. M., Spin-up from rest in a stratified fluid: boundary flows, *J. Fluid Mech.*, 472, 51–82, 2002.
- [21] Flór J.-B., Bush J. W. M. and Ungarish M., An experimental investigation of spin-up from rest of a stratified fluid, *Geophys. Astrophys. Fluid Dyn.*, 98, 277–296, 2004.
- [22] Gostiaux L. and Dauxois T., Laboratory experiments on the generation of internal tidal beams over steep slopes, *Phys. Fluids*, 19, 028102, 2007.
- [23] Zhang H. P., King B. and Swinney, H. L., Resonant generation of internal waves on a model continental slope, *Phys. Rev. Lett.*, 100, 244504, 2008.